Highly Nonlinear Photodamage in Two-Photon Fluorescence Microscopy

Alexander Hopt and Erwin Neher

Max-Planck-Institut für biophysikalische Chemie, Department of Membrane Biophysics, D-37077 Goettingen, Germany

ABSTRACT   Two-photon fluorescence excitation is being increasingly used in laser scan microscopy due to very low photodamage induced by this technique under normal operation. However, excitation intensity has to be kept low, because nonlinear photodamage sets in when laser power is increased above a certain threshold. We studied this kind of damage in bovine adrenal chromaffin cells, using two different indicators of damage: changes in resting $[Ca^{2+}]$ level and the degranulation reaction. In agreement with previous studies, we found that, for both criteria, damage is proportional to the integral (over space and time) of light intensity raised to a power ≈ 2.5. Thus, widening the laser pulse shape at constant average intensity both in time and in focal volume is beneficial for avoiding this kind of damage. Both measures, of course, reduce the two-photon fluorescence excitation. However, loss of signal can be compensated by increasing excitation power, such that, at constant damaging potential, signals may be even larger with long pulses and large focal volumes, because the exponent of the power law of damage is higher ($\mu \approx 2.5$) than that of the two-photon signal ($\mu \approx 2$).

INTRODUCTION

Reduced photodamage is widely acknowledged as one of the main advantages of two-photon excitation in laser scan microscopy on biological specimens (Denk et al., 1990; Denk and Svoboda, 1997). However, for 100–300-fs pulses, it has also been noted repeatedly that cells tend to lyse (König et al., 1995, 1996a, 1997, 1999), or show other signs of massive damage after a relatively small number of scans, if excitation intensity at the specimen plane is increased above 10 mW (Koester et al., 1999). Damage induced during two-photon laser scanning has been studied using various criteria for damage, such as red blood cell lysis (König et al., 1996b) and the ability of cells to divide after exposure (König et al., 1997). More recently, Koester et al. (1999) have studied in detail a slow rise in basal fluorescence, which occurs over time spans of minutes when neuronal dendrites are repetitively scanned over periods of minutes. In our work with brain slices using a custom-built two-photon microscope (Tan et al., 1999), we noticed that Ca^{2+} signals sometimes abruptly rose, when laser powers >10 mW were used. In bovine adrenal chromaffin cells, such abrupt changes can be observed, too. In these cells they go along with characteristic morphological changes, most likely representing the degranulation reaction, in which the cells normally release catecholamines in response to physiological stimuli. This reaction can be observed in detail with special techniques of video microscopy (Terakawa et al., 1991). However, its onset is also noticeable under normal bright field illumination. We chose to study cell damage, using both abrupt changes in basal $[Ca^{2+}]$, as measured by the fluorescence indicator dye FURA-2, and the morphological changes as criteria for damage. Using a laser pulse width of 190 fs, a wavelength of 840 nm and a pulse repetition rate of 82 MHz as default parameters, we exposed cells to repeated scans and varied beam and scan parameters, such as average light intensity, pulse duration, excitation volume (beam width of the laser at the back focal plane) and scan speed. We analyzed the data using the assumption that, at any given moment during which the focal volume is located within the cell, the probability of occurrence of damage is proportional to the spatial and temporal integral over excitation intensity raised to the power of μ. We found that a value of $\mu \approx 2.5 \pm 0.2$ satisfactorily described the data, both when observing Ca^{2+}-signals and morphological changes. Both criteria resulted in similar damage thresholds, although indicator dye was present in the cells during Ca^{2+} measurement, whereas this was not the case for the measurements using morphology as criterion. This indicates that excitation of an exogenous fluorophor is not a major cause for the photodamage revealed by the two kinds of criteria.

MATERIALS AND METHODS

Bovine adrenal chromaffin cells, grown on glass cover slips were placed into an experimental chamber and observed using a custom-built upright two-photon microscope with a 63×0.9 na water immersion objective (Achroplan, Zeiss, Jena, Germany). The microscope is described in detail by Tan et al. (1999). Briefly, it uses a Tsunami Ti:sapphire laser, pumped by a Millennia solid-state laser (both Spectra Physics, Mountain View, CA) and was built on the body of an Axioplan 2 microscope (Zeiss). Fluorescence light was separated from excitation light by a dichroic mirror immediately behind the objective and diverted either to a photomultiplier (Thorn EMI Model 9658A, Ruislip, UK) or to a CCD camera (Till Photonics, Planegg, Germany).

Cells were scanned repeatedly at 840 nm and the number of scans until appearance of signs of damage was counted. Intervals between scans were between one and two seconds. Other scan parameters will be given in the section on analysis below.

Two criteria for photodamage were used in two separate types of experiment:

- The "degranulation criterion": Distinct morphological changes, as described in the introduction, were used to judge the onset of damage. In this type of experiment, bright field images of the field of view were taken, one per laser scan frame, using a CCD camera (the laser scan image was useless in this case).
- The "FURA criterion": Sudden decreases in the indicator dye fluorescence were evaluated on the basis of a continuous (frame-by-frame) recording of two-photon fluorescence. In this type of experiment, bright field illumination was switched off; the cells had been loaded with the membrane-permeable form of the Ca^{2+}-indicator dye FURA-2 (see below) and two-photon fluorescence was excited at 840 nm. Figure 1 plots the time course of fluorescence from individual cells. It is seen that fluorescence suddenly drops after about 45 scans, indicative of a sudden $[Ca^{2+}]$ rise.

The cells used to determine photodamage according to the degranulation criterion were not loaded with FURA-2-AM. We counted the number of frames m_{degran} for the degranulation experiments and m_{FURA} for the fluorescence experiments, respectively, until the first indication of damage. For the $[Ca^{2+}]$ measurements, a sudden drop of fluorescence by at least 20% was taken as evidence for damage. Between one and five measurements were made on separate cells for each set of parameters and averages were calculated. The beam parameters, which were not varied in a particular experiment, were as typically used by workers in the field (overillumination of the pupil; objective $na = 0.9$; laser pulse half width 190 fs; 82-MHz pulse repetition rate; beamtime on the cell of interest per scan ~10 msec, 840 nm excitation wavelength). For high values of excitation intensity (>40 mW laser power at the sample) damage quite often occurred during the first scan. In the case of experiments using the $[Ca^{2+}]$ criterion, sudden increases in $[Ca^{2+}]$ could then be observed while the scan was being performed. Partial scan numbers were calculated in these cases by estimating from the scanned images the fraction of the cellular area at low $[Ca^{2+}]$.

If the laser power was decreased below a certain level, the "tolerable level," we hardly ever saw any of the above reactions within typically 1000 scans. We determined the tolerable level to be about 2.5 mW for the calcium criterion and 3 mW for the degranulation criterion.

Cell preparation and solutions

The cells were prepared according to Smith (1999). During the experiments, the cells were maintained in a chamber perfused with a saline (pH
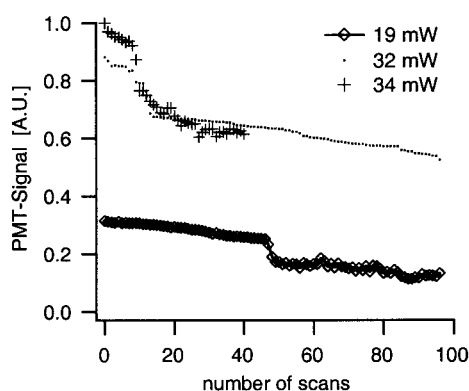

FIGURE 1   FURA-2 fluorescence of three different cells, excited at 840 nm as a function of time (number of scans m). The fluorescence was measured for each scan by acquiring an image with the PMT, choosing a region of interest in the cytoplasm with a size of ~100 pixels (0.25 μm^2 each). After a certain number of scans, the fluorescence of FURA-2, hence the PMT-signal, dropped suddenly below the 80% level of the preceding intensity. This drop in fluorescence can be explained with a rising concentration of free Ca^{2+} ions.

adjusted to 7.4 with NaOH) of (in mM) 145 NaCl, 2.5 KCl, 2.0 $CaCl_2$, 1.0 $MgCl_2$, 10.0 HEPES. To support metabolism, 2 g/l glucose were added, resulting in a final osmolarity of 296–300 mosmol/kg.

We loaded the cells with Ca^{2+}-indicator dye by the technique described by Haugland (1996). For preparing the stock solutions (1 mM), we dissolved an aliquot of 50 μg FURA-2-AM (Molecular Probes, Leiden, The Netherlands) in dry DMSO. The actual working solution (2 μM FURA-2-AM) was prepared by diluting the stock with the perfusion solution and subsequent sonication (2 min).

Measurement of the parameters expected to influence the degree of photodamage

Time-averaged power $\langle P(t) \rangle = P$

The incident power was measured in front of the scan mirrors by a calibrated photodiode (Melles Griot 13 PDH 001, Irvine, CA) with a relative error of 5%. In separate experiments, we determined that 33% of this power is lost along the optical path within the microscope up to the back focal plane of the objective. The objective itself attenuated the light by 60% in case of underillumination of the back focal plane. Further reduction occurred in standard operation when the pupil of the objective was overilluminated for optimum resolution. All power values stated here refer to power at the specimen plane, as calculated from the power reading and the corrections mentioned here.

Wavelength λ

The wavelength was measured using a grating monochromator (Jobin, Yvon, France), which was calibrated with a 632-nm HeNe-laser. The precision of this instrument is $\sim \Delta \lambda = \pm 5$ nm.

Pulse width τ

The length of the laser pulses at the sample was determined with the technique of in situ autocorrelation (Diels and Rudolph, 1996), as described in Tan et al. (1999).

Excitation volume

We measured the radius of the incident beam at the back focal plane with a small CCD-camera (Monacor TVCCD-200, Bremen, Germany). This camera was mounted on the objective revolver so that its chip was located at the back focal plane (bfp) when the corresponding revolver position was selected. To protect the CCD against the high laser power, we put a 1-mm BG39 (Schott, Mainz, Germany) filter in front of it, which decreased the radiation by a factor of $\sim 10^5$. The beam diameter then was defined as the distance between the points $\pm 1/e^2$ in a normalized intensity distribution (according to Xu and Webb, 1996). We could measure the radius with a precision of ~3 CCD-pixels, corresponding to $\Delta r = \pm 0.04$ mm.

ANALYSIS

For the analysis, we made the assumption that damage manifests itself when some noxious substance generated at rate r_D, whenever the focus resides inside the cell of interest, surpasses a certain threshold ΔP,

$$\Delta P = r_D \cdot t_c \cdot m, \qquad (1)$$

where t_c is the time that the laser focus spends inside the cell during one scan, and m is the number of scans until damage occurs. With the pixel dwell time t_{rel} (in seconds per pixel) and the scanned area of the cell A_c (in

pixels) we can write

$$t_c = t_{rel} \cdot A_c \rightarrow \frac{1}{m} = \frac{A_c}{\Delta P} \cdot t_{rel} \cdot r_D. \tag{2}$$

If we assume r_D to be proportional to the temporal mean with respect to a femtosecond-pulse cycle (indicated by $\langle \cdots \rangle$) of the spatial integral over the focal volume of light intensity raised to the μth power, we get

$$r_D = \alpha \cdot \left\langle \int_{\Delta V} dV \, I^\mu(\mathbf{r}, t) \right\rangle, \tag{3}$$

where α is a proportionality constant. The spatial integration extends over the focal volume ΔV (details and complications during beam entry into and exit from the cell are neglected).

Alternatively, we considered that the destructive event is a stochastic process occurring with probability $(1 - \exp(-r_D \Delta t))$ for time intervals Δt during which the beam resides inside the cell. However, the Poisson-like statistics of waiting times until damage, expected for such a model, could not be confirmed experimentally. We follow the treatment of similar integrals by Xu and Webb (1996) and write $I(\mathbf{r}, t)$ as a product,

$$I(\mathbf{r}, t) = I_0(t) \cdot S(\mathbf{r}), \tag{4}$$

where $S(\mathbf{r})$ represents a unitless spatial distribution function. Therefore,

$$\left\langle \int_{\Delta V} I^\mu(\mathbf{r}, t) \, dV \right\rangle = \langle I_0^\mu(t) \rangle \cdot \int_{\Delta V} S^\mu(\mathbf{r}) \, dV. \tag{5}$$

The factor g used by Xu and Webb (1996) is replaced here by a more general expression g_μ, representing μth-order coherence (Loudon, 1983),

$$g_\mu = \frac{\langle I_0^\mu(t) \rangle}{\langle I_0(t) \rangle^\mu} = \frac{g_{\mu,p}}{(f \cdot \tau)^{\mu-1}}, \tag{6}$$

where f and τ represent the repetition frequency and the pulse width (FWHM), respectively, whereas $g_{\mu,p}$ is defined as the constant factor

$$g_{\mu,p} = \frac{\int_{-1/2f}^{1/2f} I_0^\mu(t) \, dt}{(\int_{-1/2f}^{1/2f} I_0(t) \, dt)^\mu} = \frac{\tau^{1-\mu} \cdot \int_{-1/2f\tau}^{1/2f\tau} I_0^\mu(t) \, dt'}{(\int_{-1/2f\tau}^{1/2f\tau} I_0(t) \, dt')^\mu}, \tag{7}$$

which depends only on the temporal profile of the pulse ($dt' = dt/\tau$). $g_{\mu,p}$ corresponds to the constant g_p of Xu and Webb (1996).

With these expressions and the constant $c(\mu)$, which indicates the form factor of the point spread function of the μth order, we can calculate the integral from above analogous to Xu and Webb (1996) (n = refractive index, NA = numerical aperture):

$$\left\langle \int I^\mu(\mathbf{r}, t) \, dV \right\rangle = \langle I_0^\mu(t) \rangle \cdot \int_V S^\mu(\mathbf{r}) \, dV$$

$$= g_\mu \cdot \langle I_0(t) \rangle^\mu \cdot \left(\frac{n \cdot \lambda^3}{NA^4} \right) \cdot c(\mu)$$

$$= \frac{g_{\mu,p}}{f^{\mu-1} \cdot \tau^{\mu-1}} \cdot \left(\frac{\pi \cdot NA^2}{\lambda^2} \right)^\mu$$

$$\cdot \langle P(t) \rangle^\mu \cdot \left(\frac{n \cdot \lambda^3}{NA^4} \right) \cdot c(\mu) \tag{8}$$

because

$$I_0(t) = \frac{\pi \cdot NA^2}{\lambda^2} \cdot P(t). \tag{9}$$

Together with Eqs. 2 and 3, we get

$$\frac{1}{m} = \frac{A_c}{\Delta P} \cdot t_{rel} \cdot r_D$$

$$= \alpha' \cdot A_c \cdot t_{rel} \cdot \frac{g_{\mu,p}}{f^{\mu-1} \cdot \tau^{\mu-1}} \cdot \left(\frac{\pi \cdot NA^2}{\lambda^2} \right)^\mu$$

$$\cdot \langle P(t) \rangle^\mu \cdot \left(\frac{n \cdot \lambda^3}{NA^4} \right) \cdot c(\mu), \tag{10}$$

where $\alpha' = \alpha/\Delta P$.

Because we want to investigate the influence of variations in the beam radius in the bfp, we introduce it by replacing NA by $r \cdot NA_0/r_0$, where NA_0 is the specified numerical aperture of the objective, and r_0 is an effective beam radius. This results in

$$\frac{1}{m} = \alpha' \cdot A_c \cdot t_{rel} \cdot \frac{g_{\mu,p}}{f^{\mu-1} \cdot \tau^{\mu-1}} \cdot \pi^\mu \cdot \left(\frac{NA_0 r}{r_0} \right)^{2\mu-4}$$

$$\cdot \frac{1}{\lambda^{2\mu-3}} \cdot n \cdot \langle P(t) \rangle^\mu \cdot c(\mu). \tag{11}$$

The first series of our experiments was performed at fixed values of

$$
\begin{aligned}
\tau &= 190 \text{ fs} \\
r &= 2.5 \text{ mm (slight overillumination)} \\
\lambda &= 840 \text{ nm} \\
t_{rel} &= 10 \text{ } \mu s/\text{pixel (length of one pixel = 0.25 } \mu m) \\
A_c &\approx 1560 \text{ pixels} \\
t_c &= t_{rel} \cdot A_c = 15.6 \cdot 10^{-3} \text{ s} \\
f &= 82 \text{ MHz} \\
r_0 &= 1.8 \text{ mm} \\
NA_0 &= 0.9 \\
n &= 1.33.
\end{aligned}
$$

In this series, we varied P, using constant beam and scan parameters and found that a value of $\mu = 2.5$ describes the data quite well (see Results section). Using this value, we obtain, for a beam with Gaussian time profile according to Eq. 7,

$$g_{2.5,p} = \frac{\tau^{1.5} \cdot \int_{-1/2f\tau}^{1/2f\tau} I_0^{2.5}(t) \, dt}{(\int_{-1/2f\tau}^{1/2f\tau} I_0(t) \, dt)^{2.5}} = 0.576. \tag{12}$$

In subsequent experiments, we varied the following parameters: Power P, the radius r of illumination in the bfp, the laser pulse halfwidth τ, and the pixel dwell time t_{rel}. Except for P, only one parameter was varied in a given experiment. The others were left at their default values given above. For these experiments, we expect, under paraxial conditions from Eq. 11 with $\mu = 2.5$,

$$\frac{1}{m} = \alpha' \cdot 4.31 \cdot 10^6 \cdot \frac{t_{rel} \cdot r \cdot \langle P(t) \rangle^{2.5}}{\tau^{1.5}}, \tag{13}$$

where $c(2.5) = 0.216$ was calculated numerically according to Sheppard (1996) and P is in mW and r is in meter. In the case of underillumination, $c(2.5)$ had to be multiplied by 0.81 according to Xu and Webb (1996), because one has to use the Gaussian spatial distribution for $S(\mathbf{r})$ instead of the diffraction limited point spread function.

Eq. 13 gives the inverse of the number of scans in terms of the parameters varied in our experiments. More generally, the product of t_{rel} and the number of pixels (contained in the numerical constant) can be given as t_c, the time that the beam spends on a given cell. Then the number of scans m until damage, assuming paraxial conditions, is given by:

$$m = \frac{1}{\alpha'} \cdot \frac{f^{1.5} r_0 \lambda^2}{t_c c(2.5) g_{2.5,p} \pi^{2.5} NA_0 n} \cdot \frac{\tau^{1.5}}{r \cdot \langle P(t) \rangle^{2.5}}, \quad (14)$$

where t_c and τ is in seconds, r is in m, and P is in mW. The constant α' $(= 4.5 \cdot 10^{-23} [m^2/mW^{2.5}s])$ will be determined in the results section.

RESULTS

First of all, we confirmed the power law for the two-photon emission rate N_{em}, given by Xu and Webb (1996), with a fluorescein solution (Lambda Physics, Goettingen, Germany) of 10-μM concentration. We used this fluorescein concentration because it turned out to be the optimum with respect to signal level and saturation (due to balance of self-absorption and other effects). The measured fluorescence intensity varied with an exponent of 2.01 as a power function of the incident laser power over the range 10–100 mW.

According to the literature, this power law is given by (Xu and Webb, 1996)

$$\langle F(t) \rangle \approx \frac{1}{2} \cdot \phi \cdot \eta_2 \cdot C \cdot \delta \cdot \frac{g_p}{f \cdot \tau} \cdot \frac{8 \cdot n \cdot \langle P(t) \rangle^2}{\pi \cdot \lambda}, \quad (15)$$

with $\langle F(t) \rangle$, the measured time-averaged photon flux; ϕ and η_2, the fluorescence collection efficiency of the system and the fluorescence quantum efficiency of the dye, respectively; C, the concentration of the dye; and δ, the two-photon absorption cross section.

Next we measured the threshold damage m_{degran} for the degranulation criterion at different values of average laser power by varying the attenuation of the incident beam with different types of neutral density filters. Care was always taken to scan the whole area of a given cell. Pulse width, pixel dwelltime, bfp radius, wavelength, and the other parameters in Eq. 1 were kept constant during these measurements (Fig. 2 A). We found the threshold damage to be proportional to P^μ with $\mu = 2.43 \pm 0.1$.

The evaluation of degranulation experiments was particularly difficult at the threshold level of damage, because it seemed that the cells were secreting only a small number of granules. We therefore concentrated our studies on the second photodamage definition based on the measurement of fluorescence intensities. The relationship of this type of damage on laser power agreed with that of the earlier measurements ($\mu = 2.52 \pm 0.2$, Fig. 2 B). Taking $\mu = 2.5$, we can calculate and compare the proportionality constant α' (Eq. 14) for both types of damage criteria. The regression lines in Figs. 2 and 3 have values of

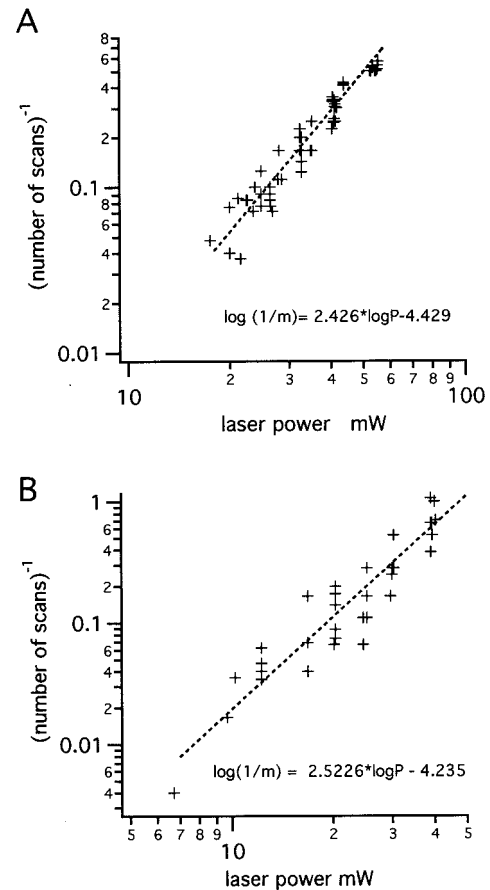$$\log\left(\frac{1}{m_{degran}}\right) - 2.43 \cdot \log P = -4.43 \pm 0.08$$

FIGURE 2 Influence of the average laser power on photodamage. The incident laser power was varied and the number (A) m_{degran} or (B) m_{fura} of scans until damage was determined using the degranulation or the FURA criterion, respectively. The remaining beam parameters from Eq. 14 were set to their default values (see text). Each symbol represents an average value from three measurements on separate dishes. The logarithm of $1/m$ was plotted against the logarithm of the power at the sample. Fits were obtained by linear regression. For the experiments in B, cells had been loaded with FURA-2-AM.

and $\quad (16)$

$$\log\left(\frac{1}{m_{FURA}}\right) - 2.52 \cdot \log P = -4.24 \pm 0.08.$$

Given the other beam parameters for the two cases (see above), we arrive at

$$\alpha'_{degran} = 2.86 \pm 1.3 \cdot 10^{-23} \left[\frac{m^2}{mW^{2.5}s}\right]$$

and

$$\alpha'_{FURA} = 4.43 \pm 1.3 \cdot 10^{-23} \left[\frac{m^2}{mW^{2.5}s}\right]. \quad (17)$$

The difference, which is hardly significant, may be caused by the fact that the FURA criterion is more sensitive, and,

therefore, photodamage due to Ca^{2+}-changes is observed at smaller intensities (cf. Fig. 2), but it may also indicate a small contribution to damage by the dye.

Additionally, it was possible to determine the influence of the temporal compression τ of the laser pulse (Fig. 3 *A*), its bfp radius r (Fig. 3 *B*) and the pixel dwelltime t_{rel} (Fig. 3 *C*). These measurements were performed by just varying one of these parameters and by determining the quantity $1/m_{FURA}$ (the "threshold damage") for different values of average laser power. Relying on the power law of damage established above ($\mu = 2.5$), we "normalized" individual m_{FURA} values by plotting mean values of $1/m(P^{2,5})$ against the variable parameter, for which we expect, according to Eq. 14, to be

$$\frac{1}{m \cdot \langle P(t)\rangle^{2.5}} \propto \frac{t_{rel} \cdot r}{\tau^{1,5}}. \qquad (18)$$

Figure 3 *A* demonstrates the dependence of damage on laser pulse width τ by a fit according to $\tau^{-1.5}$. Figure 3 *B* shows by linear regression the linear dependence between $1/mP^{2.5}$ and the bfp beam radius (as long as $2 \cdot r < d_{pupil} = 3.6$ mm) and Fig. 3 *C* confirms the linear dependence of damage on t_{rel}.

The corresponding values for the proportionality constant can be calculated from the values of the fits of Fig. 3 (in the same way as for Eqs. 16 and 17),

$$\alpha'_{FURA,\tau} = 4.47 \pm 1.3 \cdot 10^{-23}\left[\frac{m^2}{mW^{2.5}s}\right],$$

$$\alpha'_{FURA,r} = 4.52 \pm 1.3 \cdot 10^{-23}\left[\frac{m^2}{mW^{2.5}s}\right], \qquad (19)$$

$$\alpha'_{FURA,t_{rel}} = 4.5 \pm 1.3 \cdot 10^{-23}\left[\frac{m^2}{mW^{2.5}s}\right].$$

Calculating the proportionality constant for Fig. 3 *B*, we multiplied the quantity $c(\mu)$ by the factor 0.81, as explained in the context of Eq. 13, because this experiment was achieved under the condition of underillumination.

DISCUSSION

There are only few systematic studies to date on photodamage in two-photon laser-scan microscopy. However, it is general experience that incident laser power at the specimen has to be limited to ~10 mW to prevent damage to the preparation. This damage seems to be quite nonlinear in nature, because, below this threshold, two-photon excitation is very favorable for cell viability, as has been pointed out repeatedly (e.g., Denk et al., 1990; Williams et al., 1994). Comparison of data about photodamage presented so far is difficult, because the criteria that define photodamage are different in different studies.
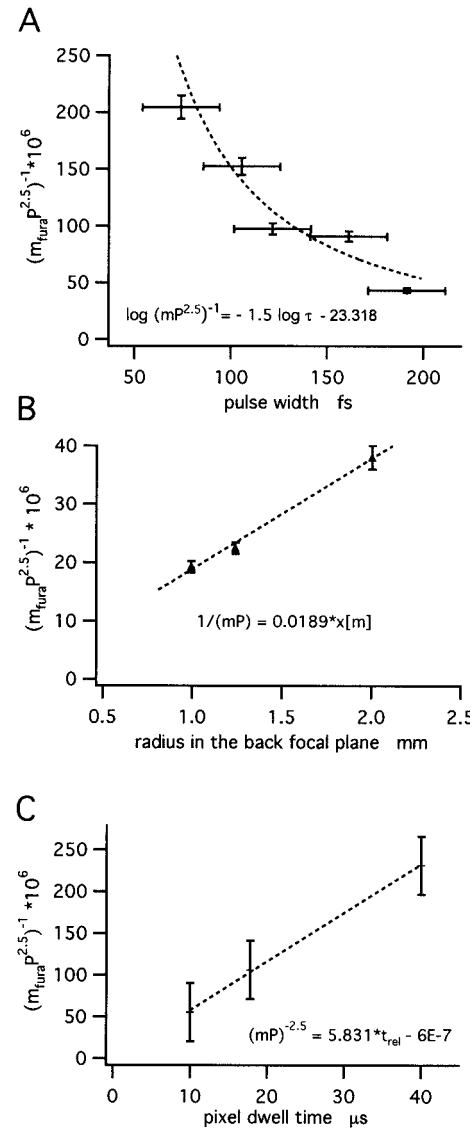

FIGURE 3. Influence of the pulse width, beam radius, and pixel dwell time on the photodamage. We measured the influence of the pulse width τ on the photodamage by varying the incident laserpower P at different values of a given parameter: (*A*) pulse width τ, (*B*) beam radius r_{bfp} in the focal plane, and (*C*) pixel dwell time t_{rel}, and determining the number m_{FURA} of scans until damage, defined by the FURA criterion. The remaining beam parameters from Eq. 14 were chosen to be constant values (see text above). Each symbol represents an average value from three measurements on separate dishes. The values of $1/(m_{FURA}P^{2.5})$ were plotted against those of the variable parameters, where P is given in mW. Fits were performed in (*B*) and (*C*) by linear regression. In (*A*), the logarithm of $1/(m_{FURA}P^{2.5})$ was separately plotted against the logarithm of the pulse width, and a fit was achieved by linear regression. (*A*) shows the resulting equation of this fit together with the data plotted against a linear abscissa. Considering the dependence of photodamage on $\tau^{-1.5}$ (Eq. 13) we obtain $1/m_{fura} \cdot P^{2.5} = 4.8 \cdot 10^{-24} \cdot \tau^{-1.5}$, and hence $\alpha'_{fura,\tau} = 4.5 \pm 1.3 \cdot 10^{-23}$. The error bars are standard deviations of the different values of $1/m_{FURA}P^{2.5}$ and the error of the measurement of pulse width (± 20 fs) in (*A*). The error in the measurement of bfp radius was ± 0.04 mm) and that of pixel dwell time was ($\pm 1.5\%$ in (*C*).

The earliest analysis of photodamage was accomplished by Ridsdale and Webb (1993) with rat basophilic leukemia cells. Cells were loaded with the calcium indicator Indo-1 and then scanned for various times at various laserpowers. It was reported that continuous scanning for up to seven minutes did not detectably kill cells at laserpowers of <50 mW, but the fraction of leaky cells increased sharply at 75 mW. Cells not loaded with dye showed a similar sensitivity to laser irradiation. Similar results were also observed with Indo-1-loaded porcine kidney epithelium-derived cells (Ridsdale and Webb, 1993). Loading the cells with the DNA binding dye HOECHST 33342 showed that there is no detectable damage at 20 mW, but a sharp transition to lethality occurs at 40–50 mW laserpower. Unfortunately, the other parameters used and the location where the power was measured are unknown, and, therefore, it is not possible to compare the results with ours.

Other experiments were carried out by König et al. (1995, 1996a, 1997, 1999), observing the cloning efficiency of Chinese hamster ovary cells or their viability measured with a live/dead fluorescence assay kit of Molecular Probes (Leiden, The Netherlands) after exposure to laser irradiation in a two-photon microscope. With the following parameters,

$$\tau = 150 \text{ fs}$$
$$na = 1.25$$
$$\lambda = 730 \text{ nm, } 760 \text{ nm, and } 800 \text{ nm}$$
$$t_{rel} = 80 \ \mu\text{s/pixel}$$
$$f = 80 \text{ MHz}$$
$$f_0 = 2.6 \text{ mm,}$$

the cells were exposed to 10 scans each and afterwards incubated for 5–6 days. With an excitation power (measured at the sample) of ≤1 mW, there was no difference in the cloning efficiency; from 6 mW onward, the cells were unable to form clones and to exclude the dead-cell indicator trypan blue. With power levels of >10 mW (10^{12} W/cm^2 = 10^{32} photons/cm^{2}s) massive cell death was observed.

Using the proportionality constant $\alpha'_{FURA} = 4.5 \pm 1.3 \cdot 10^{-23} [m^2/mW^{2.5}s]$ of our study, Eq. 14, and the parameters given above, we can calculate the power, which should cause damage after 10 scans. The result, 7.1 mW for the excitation wavelength 800 nm (closest to the wavelength we used), quite accurately predicts the value of the damage threshold found in Chinese hamster ovary cells. Further, König et al. (1996a) needed more power to achieve the same decreases in cloning efficiencies if they increased the laser wavelength. This result is consistent with our Eq. 14. With smaller structures, like axonal varicosities, we typically can use somewhat higher powers up to about 10 mW without causing serious damage (Tan et al., 1999). This is consistent with the equations given above, because the number of scans at a given scan speed is predicted to be proportional to the cellular projection area (if the focal depth is smaller than the extension of the cell in the z-direction). Thus, for an axonal varicosity, with typical cross section of ≈40 μm^2,

the possible number of scans should be about 4 times larger than for a chromaffin cell, with typically 175 μm^2. Also, it should be noted that, in all of our measurements, we used continuous scanning at rates of about 2 per second. If, as assumed in our analysis, damage is due to the build-up of a noxious substance, it is well conceivable that slower scanning, or scanning with intermittent pauses is less damaging, because the noxious substance may dissipate or be degraded by repair mechanisms.

Recently, Koester et al. (1999) examined a more subtle type of damage in neocortical neurons, which is a slow, cumulative increase in fluorescence, when a given site is scanned repetitively. We noticed such an effect in our experiments at excitation powers slightly below those that cause the destructive photodamage that underlies our damage criteria. Koester et al. found a power law with an exponent of 2.5 for the rate of fluorescence increase, and they studied the dependence of this kind of damage on laser pulse width (see below). Comparing all studies on damage effects published so far, it can be concluded that quite a variety of damage processes set in at similar power levels with similar exponents in different cell types.

Our results indicate that destructive photodamage of biological samples is caused by a multiphoton process, maybe a mixture of two- and three-photon absorption, or by a two-photon absorption followed by partially saturated secondary process. In agreement with Koester et al. (1999), we suggest that, at low excitation intensities, damage may be dominated by a two-photon absorption process, but higher order mechanisms will become important at larger excitation powers. This conclusion is also compatible with the calculations of Schönle and Hell (1998), who state that no significant one-photon absorption takes place at wavelengths similar to the ones used in two-photon microscopy. The generation of heat is therefore not a mechanism that can explain the photodamage (Schönle and Hell, 1998; König et al., 1996b). A possible alternative is the damage due to extremely high fields and hence destructive intracellular optical breakdown (Brakenhoff et al., 1995; König et al., 1996b). Plasma formation by femtosecond laser pulses has been reported in other nonorganic materials at similar intensities (von der Linde and Schüler, 1996).

If absorption plays a role in photodamage, three-photon absorption seems to be particularly relevant. This is conceivable, if one considers the corresponding one-photon wavelength range for a three-photon absorption with our laser system. Exciting with 800–900 nm laserlight, a three-photon absorption corresponds to a one-photon absorption around 200–300 nm. According to Clayton (1977), light with this wavelength is absorbed maximally by cellular DNA and proteins. Hence, it has a high damage potential, although three-photon-absorption should not occur frequently considering the laser parameters we used. This may also explain why the degradation of the cloning efficiency (possible damage of DNA) and the rise of Ca^{2+} levels

(possible damage of proteins, which regulate the Ca^{2+} currents) happen at similar power levels.

Safe limits for standard operation

For beam parameters typically used by workers in the field (overillumination of the pupil; objective $na = 0.9$; laser pulse half width 150 fs; 82-MHz pulse repetition rate; beamtime on the cell of interest per scan = 10 msec, 800-nm excitation wavelength), we expect the average number of scans m_{FURA} before damage occurs to be about 2500 at 2.5 mW laser power (in the specimen plane). At 10 mW laser power, we calculate $m_{FURA} = 77$. Thus, 2.5 mW can be considered to represent a "safe" working condition for typical experiments, unless thousands of images are being taken routinely. Considering Eqs. 14 and 15, one can ask the question, what changes in signal intensity can be expected if beam parameters are changed in a way that leaves the damaging potential constant?

Substituting the power $P(t)$ in Eq. 15 by that obtained for a fixed m-value (from Eq. 14), it is concluded that the fluorescence signal at damage threshold varies with $\tau^{0.2}/r^{0.8}$. Thus, our results predict a small increase in signal when the laser pulse width is lengthened and power is simultaneously increased in a way that damaging potential stays constant. This, however, is a small effect, and it depends critically on the exponent (-1.5) of the fit to the data (Fig. 3 *A*) regarding pulse-length variations (which has an accuracy of ± 0.7). Two recent studies (König et al., 1999; Koester et al., 1999) addressed the problem of pulse-length variation and found a constant fluorescence signal at damaging threshold, indicating that the damaging effect has the same exponent as fluorescence excitation. Also, two-photon microscopy with laser pulses in the picosecond range (Bewersdorf and Hell, 1998) and even with continuous wave excitation has been demonstrated (Hell et al., 1998; Booth and Hell, 1998). However, for very long pulses and high excitation energies, other factors, like fluorescence saturation, heat generation in water (Schönle and Hell, 1998) or maximum available laser power may be limiting. These results are compatible with our measurements, given the standard error of our estimate for the exponent. They demonstrate that, under a large variety of conditions, the fluorescence signal changes only little with pulse width, if total power is adjusted for similar damaging potential. It should be understood, though, that our equations predict a substantial increase in signal when the focal volume is enlarged by reducing the incident beam radius r (resulting in underillumination of the bfp). This will degrade resolution, particularly in the z-direction. However, in many applications of two-photon-fluorescence microscopy, particularly for fast Ca^{2+} imaging, signal level and its associated shot noise is a severely limiting factor (Tan et al., 1999), and spatial resolution is compromised anyway by diffusion of indicator dyes during a scan frame. In these cases, the signal may not be degraded when underilluminating the bfp and when using relatively long laser pulses. If, in such cases, the specimen is sufficiently thick, such that the widely extended focal volume (in the z-direction) can contribute to fluorescence, the signal may be even improved with underillumination, contrary to the often-held view that very short and well-focused pulses are best for two-photon microscopy.

REFERENCES

Bewersdorf, J., and S. W. Hell. 1998. Picosecond pulsed two-photon imaging with repetition rates of 200 and 400 MHz. *J. Microsc.* 191: 28–38.

Booth, M., and S. W. Hell. 1998. Continuous wave excitation two-photon fluorescence microscopy exemplified with the 647 nm ArKr laser line. *J. Microsc.* 190:298–304.

Brakenhoff, G. J., M. Müller, and J. Squier. 1995. Femtosecond pulse width control in microscopy by two-photon absorption autocorrelation. *J. Microsc.* 179:253–260.

Clayton, R. K. 1977. Light and Living Matter—A Guide to the Study of Photobiology, Vol. 1 and 2. McGraw-Hill, New York.

Denk, W., J. H. Strickler, and W. W. Webb. 1990. Two-photon laser scanning fluorescence microscopy. *Science.* 248:73–76.

Denk, W., and K. Svoboda. 1997. Photon upmanship: why multiphoton imaging is more than a gimmick. *Neuron.* 18:351–357.

Diels, J. C., and W. Rudolph. 1996. Ultrashort Laser Pulse Phenomena. Academic Press, London.

Haugland, R. P. 1996. Handbook of Fluorescent Probes and Research Chemicals. Molecular Probes, Leiden, The Netherlands. 549–550.

Hell, S. W., M. Booth, S. Wilms, C. M. Schnetter, A. K. Kirsch, D. J. Arndt-Jovin, and T. M. Jovin. 1998. Two-photon near- and far-field fluorescence microscopy with continuous-wave excitation. *Optics Lett.* 23:1238–1240.

Koester, H. J., D. Baur, R. Uhl, and S. W. Hell. 1999. Ca^{2+} fluorescence imaging with pico- and femtosecond two-photon excitation: signal and photodamage. *Biophys. J.* 77:2226–2236.

König, K., H. Liang, M. W. Berns, and B. J. Tromberg. 1995. Cell damage by near-IR microbeams. *Nature.* 377:20–21.

König, K., H. Liang, M. W. Berns, and B. J. Tromberg. 1996a. Cell damage in near-infrared multimode optical traps as a result of multiphoton absorption. *Optics Lett.* 21:1090–1091.

König, K., U. Simon, and K. J. Halbhuber. 1996b. 3D resolved two-photon fluorescence microscopy of living cells using a modified confocal laser scanning microscope. *Cell. Mol. Biol.* 42:1181–1194.

König, K., P. C. T. So, W. W. Mantulin, and E. Gratton. 1997. Cellular response to near-infrared femtosecond laser pulses in two-photon microscopes. *Optics Lett.* 22:135–136.

König, K., T. W. Becker, P. Fischer, I. Riemann, and K.-J. Halbhuber. 1999. Pulse-length dependence of cellular response to intense near-infrared laser pulses in multiphoton microscopes. *Optics Lett.* 24: 113–115.

Loudon, J. 1983. The Quantum Theory of Light. Oxford University Press, London.

Ridsdale, J. A., and W. W. Webb. 1993. The viability of cultured cells under two-photon laser scanning microscopy (abstr.). *Biophys. J.* 64: A109.

Schönle, A., and S. W. Hell. 1998. Heating by absorption in the focus of an objective lens. *Optics Lett.* 23:325–327.

Sheppard, C. J. R. 1996. Image formation in three-photon fluorescence microscopy. *Bioimaging.* 4:124–128.

Smith, C. 1999. A persistent activity-dependent facilitation in chromaffin calls is caused by Ca^{2+} activation of protein kinase C. *J. Neurosci.* 19:589–598.

Tan, Y. P., I. Llano, A. Hopt, F. Würriehausen, and E. Neher. 1999. Fast scanning and efficient photodetection in a simple two photon microscope. *J. Neurosci. Methods.* 92:123–135.

Terakawa, S., J.-H. Fan, K. Kumakura, and M. Ohara-Imaizumi. 1991. Quantitative analysis of exocytosis directly visualized in living chromaffin cells. *Neurosci. Lett.* 123:82–86.

von der Linde, D., and H. Schüler. 1996. Breakdown threshold and plasma formation in femtosecond laser-solid interaction. *J. Opt. Soc. Am. B.* 13:216–222.

Williams, R. M., D. W. Piston, and W. W. Webb. 1994. Two-photon molecular excitation provides intrinsic 3-dimensional resolution for laser-based microscopy and microphotochemistry. *FASEB J.* 8:804–813.

Wilson, T., and C. J. R. Sheppard. 1984. Theory and Practice of Scanning Optical Microscopy. Academic Press, London.

Xu, C., and W. W. Webb. 1996. Measurement of two-photon excitation cross sections of molecular fluorophores with data from 690 to 1050 nm. *J. Opt. Soc. Am. B.* 13:481–491.